VOL. 16, NO. 18, SEPTEMBER 2021 ISSN 1819-6608
ARPN Journal of Engineering and Applied Sciences

www.arpnjournals.com

SORET AND DUFOUR EFFECTS ON MHD TRANSIENT FLOW OVER AN EXPONENTIALLY ACCELERATED PLATE WITH RAMPED TEMPERATURE

S. Jayaprasad[1], Siva Reddy Sheri[2], D. Mahendar[3] and Anjan Kumar Suram[3]
[1]Department of Mathematics, Girraj Govt. Degree College (A), Nizamabad, Telangana, India
[2]Department of Mathematics, GITAM University, Hyderabad Campus, Telangana, India
[3]Department of Mathematics, B V Raju Institute of Technology, Narsapur, Telangana, India
E-Mail: sreddy7@yahoo.co.in

ABSTRACT

This article deals with the effects of Soret and Dufour on MHD transient flow over an exponentially accelerated plate with ramped temperature. The dimensional flow governing equations associated with boundary conditions are converted to non-dimensional form. These converted equations are solved for numerical solutions by using Finite element technique. To understand the influence of individual emerging flow pertinent parameters, obtained results are depicted and illustrated in depth with the aid of graphs. Tabulated representation is used to exemplify the variations in skin frictions, Nusselt number and Sherwood number against different parameters. In a special case acquired computational results are compared with the existing literature and a satisfactory coordination is achieved.

Keywords: soret and dufour effects, MHD, ramped temperature, FEM.

INTRODUCTION

Magneto hydrodynamics (MHD) is the investigation of electrically conducted liquids which are being with magnetic field. Magnetic field impacts are normal and man-made flows. They are commonly used in industry to pump, heat, levitate and stir liquid metals. There is the earthbound attractive field which is kept up by smooth motion in the world's canter, the daylight based attractive field which makes sunspots and sun-based flares, and the galactic magnetic field which impacts the formation of stars. In any case, there was some early leading work by the specialist J. Hartmann, who designed the electromagnetic pump in 1918. Hartmann additionally undertook an efficient hypothetical and test examination of the progression of mercury in a homogeneous magnetic field. In the preface to the 1937 paper depicting his investigation and observation. The implementation of MHD in engineering was progressively moderate less get going until the 1960s. Later extraordinary work has done by different analysts, some of them are Anwer Beg *et al.* [1] have discussed computation of non-isothermal thermo-convective micropolar liquid elements in a Hall MHD generator framework with non-direct distending wall. Veeresh *et al.* [2] studied MHD radiative Casson fluid with Joule heating and thermal diffusion. Satya Narayana *et al.* [3] described chemical reaction and heat source effects on MHD oscillatory flow in an irregular channel. Makinde [4] examined heat and mass exchange by MHD mixed convection stagnation point flow to a vertical plate inserted in a highly porous medium with radiation and internal heat generation. Bhaskar *et al.* [5] studied MHD natural convection flow past a moving vertical plate with ramped temperature. Bhaskar *et al.* [6] have found finite element approximation of MHD flow past a vertical plate in an embedded porous medium with a convective boundary condition and cross diffusion. Bhaskar *et al.* [7] discussed Numerical analysis of MHD Casson fluid flow over an exponentially accelerated vertical plate in embedded porous medium with ramped wall temperature and ramped surface concentration in uniform magnetic field. Jena *et al.* [8] studied chemical reaction effect on MHD Jeffery fluid flow over a stretching sheet through porous media with heat generation/absorption.

Heat is the transport of energy from higher region to lower. If there is any temperature difference in the system or two systems with different temperatures are brought into thermal contact, then heat transfer takes place. Energy travel cannot be observed or measured directly, but the influence generated by it can be identified. Because transformation of heat involves energy conversion. The transformation of heat satisfies first and second laws of thermodynamics. Similarly, transportation of an individual chemical species from a region of high concentration to low is known as mass transfer. Heat and mass transfer are a natural phenomenon which occurs frequently in many practical situations; sometimes heat transfer happens individually and sometimes occurs along with mass transfer. It has numerous geophysical and engineering applications such as cooling of nuclear reactors, drying of porous solids, enhanced oil recovery, geothermal reservoirs, packed-bed catalytic reactors, thermal insulation and underground energy transport. The pioneering work relevant to this area is Seth *et al.* [9] investigated the analytical influence of Hall current on magneto hydro dynamic free convective heat and mass transfer flow of rotating fluid past a vertical plate with ramped temperature. Bhargava *et al.* [10] have discussed the effect of Rayleigh number on nonlinear convective heat and mass transfer in a micro polar fluid-filled enclosure using FEM. Pal and Mondal [11] have analysed the influence of Soret-Dufour effects and chemical reaction on MHD non-Darcian mixed convection heat and mass transfer over a non-linear stretching sheet.

ARPN Journal of Engineering and Applied Sciences

In most of the researches numerical or analytical results are found by assuming the constraints for the movement, heat and concentration at the plate are continuous and well defined. Nevertheless, there are different problems which may necessitate changing conditions, by considering this fact, numerous authors studied different flows with step change in the surface temperature. Siva Reddy Sheri *et al*. [12] investigated the effect of viscous dissipation on natural convection flow past an impulsively moving vertical plate with ramped temperature. Siva Reddy Sheri *et al*. [13] have discussed the impact of chemical reaction and Hall current free convective flow past an accelerated moving vertical plate with ramped temperature using finite element analysis. Siva Reddy Sheri *et al.* [14] have analyzed Soret- Dufour effects on MHD natural convective flow through porous medium in a rotating system with ramped temperature. Siva Reddy Sheri and Anjan Kumar Suram [15] have investigated finite element analysis of heat and mass transfer past an impulsively moving vertical plate with ramped temperature. Mahendar and Srikanth Rao [16] have discussed unsteady MHD free convection and mass transfer flow past a porous vertical plate in the presence of viscous dissipation.

Aforementioned research works motivated us to analyse the effect of Soret and Dufour on MHD transient flow over an exponentially accelerated plate with ramped temperature. In the current probe the numerical results of governing equations are obtained by finite element method and the influence of several pertaining parameters are illustrated through graphs and tables. The numerical results are compared with skin frictions, Nusselt number and Sherwood number and found to be in good agreement with previous results as special case of (in the absence of viscous dissipation, Soret and Dufour parameters) the present investigation.

FORMULATION OF THE PROBLEM

Consider an unsteady magnetohydrodynamic natural convective stream of an incompressible electrically conducting, viscous, chemically reactive, optically thin radiating and heat absorbing fluid past an exponentially accelerated moving vertical plate of infinite extent with ramped wall temperature, embedded in a uniform porous medium taking Hall current and rotation into account. Cartesian co-ordinate system (x', y', z') is chosen in such a way that x' -axis is taken in upward along with vertical plate, y'-axis is normal to the plate and z' -axis is perpendicular to $x'y'$plane. The fluid flow is assumed to be parallel to y'-axis under the influence of a uniform magnetic field B_0 both the fluid and the plate rotate in anticlockwise direction about y'-axis with a uniform angular velocity Ω'. At the start i.e. at time $t' \leq 0$, both the fluid and the plate are kept at rest with uniform temperature and concentration $T'_\infty$and C'_∞ respectively. After some time i.e at time $t' > 0$, plate started moving exponentially with velocity $U_0 e^{b't'}$ in x'-direction (U_0 being characteristic velocity). The temperature of the plate is raised or lowered to $T'_\infty + (T'_w - T'_\infty)t'/t_0$when $0 < t' < t_0$ is maintained at uniform temperature T'_w thereafter i.e. when $t' > t_0$. Also, at time $t' > 0$, the species concentration is elevated to a uniform species concentration C'_w and is maintained thereafter. It is presumed that a uniform chemical reaction of order one ensues with a constant rate K'_r between the fluid and dispersing species.

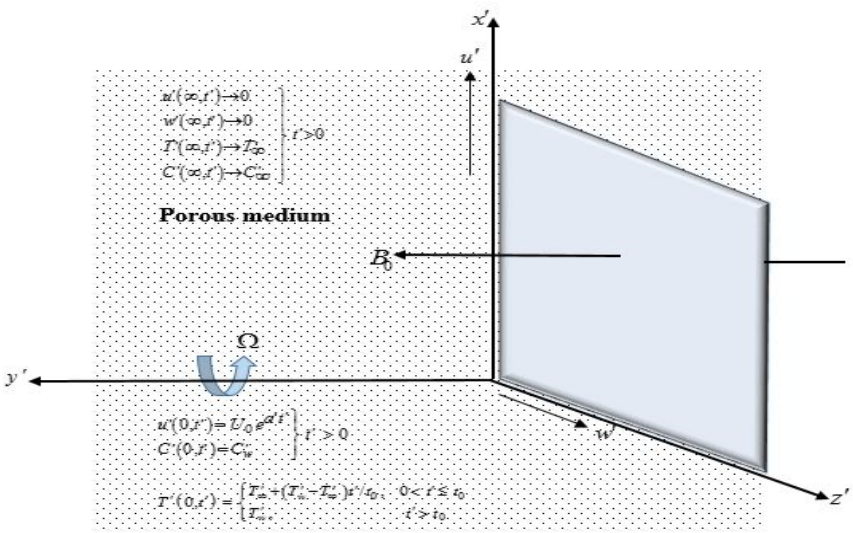

Figure-1. Physical model and coordinate system.

In the current investigation fluid is partially ionized or metallic liquid with very small magnetic Reynolds number. Thus, the induced magnetic field due to the fluid flow is insignificant in comparison to the applied one (Cramer and Pai [17]). Hence, the magnetic field becomes $\vec{B}_0 = (0, B_0, 0)$ Since, the plate is infinite in x' and z' directions, all physical parameters excluding pressure are dependent on $y'$and t'.

By keeping above assumptions into consideration, the equations presiding the unsteady magneto hydro dynamic transient flow of an optically thin heat radiating, incompressible, viscous, chemically reactive, temperature dependent heat absorbing/generating and electrically conducting fluid past an exponentially accelerated infinite vertical plate having ramped temperature in a porous medium considering the effects of Hall current and rotation under the approximation proposed by Boussinesq,

$$\frac{\partial u'}{\partial t'}+2\Omega' w'=\upsilon\frac{\partial^2 u'}{\partial y'^2}-\left(\frac{\sigma B_0^2}{\rho}\right)\frac{(u'+mw')}{(1+m^2)}-\frac{\upsilon}{K'}u' +g\beta'\left(T'-T'_\infty\right)+g\beta^*(C'-C'_\infty) \quad (1)$$

$$\frac{\partial w'}{\partial t'}-2\Omega' u'=\upsilon\frac{\partial^2 w'}{\partial y'^2}+\left(\frac{\sigma B_0^2}{\rho}\right)\frac{(mu'-w')}{(1+m^2)}-\frac{\upsilon}{K'}w' \quad (2)$$

$$\frac{\partial T'}{\partial t'}=\frac{k}{\rho c_p}\frac{\partial^2 T'}{\partial y'^2}-\frac{Q_0}{\rho c_p}\left(T'-T'_\infty\right)-\frac{1}{\rho c_p}\frac{\partial q'_r}{\partial y'} +\frac{\upsilon}{\rho c_p}\left(\frac{\partial u'}{\partial y'}\right)^2+\frac{D_m k_T}{c_s c_p}\frac{\partial^2 C'}{\partial y'^2} \quad (3)$$

$$\frac{\partial C'}{\partial t'}=D_m\frac{\partial^2 C'}{\partial y'^2}+\frac{D_m k_T}{T_m}\frac{\partial^2 T'}{\partial y'^2}-k'_r C' \quad (4)$$

Associated initial and boundary conditions for the present investigation are given as

$$\left|\begin{array}{l} u'=w'=0, T'=T'_\infty, C'=C'_\infty \ for\ \ y'\geq 0\ and\ t'\leq 0,\\ u'=U_0 e^{b't'}, w'=0, C'=C'\ at\ y'=0\ \ for\ t'>0,\\ T'=T'_\infty+\left(T'_w-T'_\infty\right)t'/t_0\ at\ \ y'=0\ \ for\ 0<t'\leq t_0,\\ T'=T'_w\ at\ y'=0\ \ for\ t'>t_0,\\ u', w'\to 0, T'\to T'_\infty,\ C'\to C'_\infty\ as\ \ y'\to\infty\ \ for\ t'>0 \end{array}\right| \quad (6)$$

Where u'- velocity of the fluid along x'- axis, w'- velocity of the fluid along z'- axis, g -gravitational acceleration, υ - kinematic coefficient of viscosity, β'- thermal expansion coefficient, β^*- coefficient of volumetric expansion, T' - temperature of the fluid, C'- concentration of the species, ρ- density of the fluid, σ- electrical conductivity, K'- permeability of porous medium, m=$\omega_e\tau_e$ - Hall current parameter, ω_e- cyclotron frequency, τ_e- electron collision time, k- thermal conductivity of the fluid, c_p- specific heat at constant pressure, D_m- molecular mass diffusivity, k'_r -chemical reaction coefficient, Q_0- coefficient of heat absorption, q'_r- radiative heat flux, k_T- thermal diffusion ratio, T_m- mean fluid temperature

Local radiant absorption for an optically thin grey fluid is presented as (Raptis, [18])

$$\frac{\partial qr'}{\partial y'}=4a^*\sigma^*(T'^4-T'^4_\infty) \quad (6)$$

Where $a^*$is absorption coefficient and $\sigma^*$is Stefan- Boltzmann constant.

It is considered that the temperature difference within the fluid flow is sufficiently small such that fluid temperature T'^4 may be expressed as a linear function of the temperature. It can be obtained by expanding T'^4 in a Taylor series about free stream temperature T'_∞. Neglecting second and higher order terms, is expressed as

$$T'^4\cong 4T_\infty'^3 T'-3T'^4_\infty \quad (7)$$

By using Equations (6) and (7) in Equation (3), we obtain

$$\frac{\partial T'}{\partial t'}=\frac{k}{\rho c_p}\frac{\partial^2 T'}{\partial y'^2}-\frac{16\delta\sigma^* T'^3_\infty}{\rho c_p}(T'-T'_\infty)-\frac{Q_0}{\rho c_p}\left(T'-T'_\infty\right) +\frac{\upsilon}{\rho c_p}\left(\frac{\partial u'}{\partial y'}\right)^2+\frac{D_m k_T}{c_s c_p}\frac{\partial^2 C'}{\partial y'^2} \quad (8)$$

Introducing non-dimensional variables and parameters

$$\left|\begin{array}{l} y=\frac{y'}{U_0 t_0}, u=\frac{u'}{U_0}, w=\frac{w'}{U_0},\ t=\frac{t'}{t_0},\ T=\frac{(T'-T'_\infty)}{(T'_w-T'_\infty)},\\ C=\frac{(C'-C'_\infty)}{(C'_w-C'_\infty)}, \Omega=\frac{\Omega'\nu}{U_0^2}, M=\frac{\sigma B_0^2\nu}{\rho U_0^2}, m=\omega_e\tau_e,\\ K=\frac{K'U_0^2}{\nu^2}, Gr=\frac{g\beta'\nu(T'_w-T'_\infty)}{U_0^3},\\ Gc=\frac{g\beta^*\nu(C'_w-C'_\infty)}{U_0^3}, \Pr=\frac{\nu c_p}{k}, R=\frac{16a^*\sigma^*\nu T'^3_\infty}{U_0^2\rho c_p},\\ Q=\frac{Q_0\nu}{\rho c_p U_0^2}, Du=\frac{D_m k_T}{c_s c_p}\frac{(C'_w-C'_\infty)}{(T'_w-T'_\infty)},\\ Sc=\frac{\nu}{D_m}, Sr=\frac{D_m k_T}{\nu T_m}\frac{(T'_w-T'_\infty)}{(C'_w-C'_\infty)},\\ Kr=\frac{k_r'\nu}{V_0^2}, Ec=\frac{U_0^2}{\rho c_p(T'_w-T'_\infty)} \end{array}\right| \quad (9)$$

Making use of equation (9) in Equations (1), (2), (8) and (4) we get non-dimensional form as

$$\frac{\partial u}{\partial t}+2\Omega w=\frac{\partial^2 u}{\partial y^2}-\left(\frac{M}{1+m^2}\right)(u+mw)-\frac{u}{K}+GrT+GcC \quad (10)$$

$$\frac{\partial w}{\partial t}-2\Omega u=\frac{\partial^2 w}{\partial y^2}+\left(\frac{M}{1+m^2}\right)(mu-w)-\frac{w}{K} \quad (11)$$

$$\frac{\partial T}{\partial t}=\frac{1}{\Pr}\frac{\partial^2 T}{\partial y^2}-RT-QT+Ec\left(\frac{\partial u}{\partial y}\right)^2+Du\frac{\partial^2 C}{\partial y^2} \quad (12)$$

$$\frac{\partial C}{\partial t}=\frac{1}{Sc}\frac{\partial^2 C}{\partial y^2}+Sr\frac{\partial^2 T}{\partial y^2}-KrC \quad (13)$$

Where u, w, K^2, b, M ,Gr, Gc,K,R, Q, Du, Ec, Sc, Sr, Kr and Pr are primary fluid velocity, secondary fluid velocity, rotation parameter, surface acceleration parameter, magnetic parameter, thermal Grashof number, solutal Grashof number, porosity parameter, radiation parameter, heat absorption parameter, Dufour number, Eckert number, Schmidt number, Soret number, chemical reaction parameter and Prandtl number respectively.

The corresponding initial and boundary conditions, presented by Equation (9) in non-dimensional form, are given by

$$\left\{\begin{array}{l} u=w=0,\ T=0, C=0 \quad for\ y\geq 0\ and\ t\leq 0, \\ u=e^{bt}, w=0, C=1\ at\ y=0 \quad for\ t>0, \\ T=t\ at\ y=0 \quad for\ 0<t\leq 1, \\ T=1\ at\ y=0 \quad for\ t>1, \\ u, w\to 0, T\to 0, C\to 0 \quad as\ y\to\infty \quad for\ t>0 \end{array}\right\} \quad (14)$$

METHOD OF SOLUTION

The FEM is a numerical technique for solving problems of engineering and mathematical physics includes structural analysis, heat transfer, fluid flow, mass transfer and electromagnetic potential. It especially deals with complicated geometries, loadings and material properties. The detailed description of this method is explained by Bathe [19] and Reddy [20]. The fundamental steps involved in FEM are.

- Divide the "infinite" fluid domain into finite number of elements.
- Derive the equations for every element.
- Assembly of Element Equations.
- Imposition of boundary conditions.
- Solution of assembled equations.

The final matrix equation obtained can be solved by iterative scheme.

A grid refinement test is carried out by dividing the whole domain into successively sized grids 81x81, 101x101 and 121x121 in the z-axis direction. Furthermore, we ran the developed code for different grid sizes and finally we found that all the solutions are independent of grid. After many tests we adopted grid size as 101 intervals. Thus all the computations were carried out with 101 intervals of equal step size 0.01. At each node 6 functions are to be evaluated and after assembly of element equations, a set of 606 non-linear equations are obtained and which may not produce closed form solutions, consequently an iterative scheme is adopted to solve the system by introducing the boundary conditions. Finally, the solution is assumed to be convergent whenever the relative difference between two successive iterations is less than the value 10^{-6}. This method has been proven to be adequate and give accurate results for boundary layer equations. Now it is important to calculate the physical quantities of primary interest, which are the Skin-friction, Wall couple stress, Nusselt number and Sherwood number.

Skin-friction is obtained as,

$$C_f=\left[\frac{\partial u}{\partial y}\right]_{y=0} \quad or \quad C_f=u'(0) \quad (15)$$

Wall couple stress is obtained as,

$$C_w=\left[\frac{\partial w}{\partial y}\right]_{y=0} \qquad C_w=w'(0) \quad (16)$$

The rate of the heat transfer in terms of the Nusselt number is given by,

$$Nu=-\left[\frac{\partial T}{\partial y}\right]_{y=0} \quad or \quad Nu=-T'(0) \quad (17)$$

The coefficient of Mass transfer, generally known as Sherwood number is given by,

$$Sh=-\left[\frac{\partial C}{\partial y}\right]_{y=0} \quad or \quad Sh=-C'(0) \quad (18)$$

VALIDATION OF NUMERICAL RESULTS

To know the truthiness and the validity of the current numerical method we made a comparison with the previously published results by Seth *et al*. [9]. A great coordination between the results exists. This comparison is expressed in the form of tables 1-4.

Table-1 shows that 'Sh' values increased with rising values of Kr and a reverse tendency is identified against t.

Tables 2 and 3 describe the influence of m, M, Ω, K Gr, Gc, R and Q on primary and secondary skin frictions for ramped temperature and isothermal plate respectively. It display that primary skin friction get accelerated on rising M, Ω, R and Q and an opposite tendency has identified for rising values of m,K,Gr, and Gc. It is also recognized from these tables that secondary

skin friction get growing against m, M, Ω, K, Gr and Gc and it decelerates on increasing R and Q.

Table-4 describes the Nusselt number values enriched against R and Q. A retarding impact is identified in Nusselt number with respect to the time for ramped temperature. For isothermal case Nu increases on increasing t.

Table-1. Comparison of Sherwood number when (*Ec*=0, *Du*=0 and *Sr*=0).

		Seth *et al.* [9]	Present Results
Kr	*t*	*Sh*	*Sh*
2.5	0.5	1.26238	1.262379
0.5	0.7	0.69519	0.695200

Table-2. Comparison of primary and secondary Skin friction values for ramped temperature when (*Ec*=0, *Du*=0 and *Sr*=0).

								Seth *et al.* [9]		Present Results	
m	*M*	Ω	*K*	***Gr***	***Gc***	***R***	*Q*	C_f	C_w	C_f	C_w
1.0	10	2	0.2	10	3	2	3	2.36605	1.78672	2.366049	1.786719
0.5	15	2	0.2	10	3	2	3	3.48712	1.51988	3.487119	1.519880
0.5	10	4	0.2	10	3	2	3	3.04024	2.02350	3.040240	2.02349
0.5	10	2	0.25	10	3	2	3	2.62812	1.48072	2.628120	1.480720
0.5	10	2	0.2	15	3	2	3	2.40519	1.48133	2.405200	1.481329
0.5	10	2	0.2	10	5	2	3	2.37894	1.51329	2.378939	1.513289
0.5	10	2	0.2	10	3	4	3	2.82225	1.41352	2.822249	1.413520
0.5	10	2	0.2	10	3	2	5	2.82225	1.41352	2.822249	1.413519

Table-3. Comparison of primary and secondary Skin friction values for isothermal plate when (*Ec*=0, *Du*=0 and *Sr*=0).

								Seth *et al.* [9]		Present Results	
m	*M*	Ω	*K*	***Gr***	***Gc***	***R***	*Q*	C_f	C_w	C_f	C_w
1.0	10	2	0.2	10	3	2	3	1.39594	2.06245	1.395939	2.062449
0.5	15	2	0.2	10	3	2	3	2.64142	1.69866	2.641420	1.698660
0.5	10	4	0.2	10	3	2	3	2.17136	2.28258	2.171359	2.282580
0.5	10	2	0.25	10	3	2	3	1.67472	1.69700	1.674719	1.697000
0.5	10	2	0.2	15	3	2	3	1.00344	1.78086	1.003440	1.780859
0.5	10	2	0.2	10	5	2	3	1.44444	1.51329	1.444439	1.513300
0.5	10	2	0.2	10	3	4	3	1.94575	1.59033	1.945749	1.590329
0.5	10	2	0.2	10	3	2	5	1.94575	1.59033	1.945750	1.590329

Table-4. Comparison of Nusselt number when (*Ec*=0, *Du*=0 and *Sr*=0).

			Seth *et al.* [9]		Present Results	
R	*Q*	*t*	**Ramped**	**Isothermal**	**Ramped**	**Isothermal**
4	3	0.5	1.27368	2.23148	1.273679	2.231479
2	5	0.5	1.27368	2.23148	1.273680	2.231480
2	3	0.7	1.50704	1.88595	1.507039	1.885949

RESULTS AND DISCUSSIONS

Finite element method is used to solve the governing equations (10)-(13) with subject to constraints (14). In order to analyze the effect of various pertinent parameters on the flow fields for both ramped temperature and isothermal plates are articulated through the graphs 2-39. The table format is presented to explain the influence of particular parameters on primary and secondary skin frictions, Nusselt number and Sherwood number.

The effect of magnetic parameter on dimensionless primary and secondary velocity fields for both ramped temperature and isothermal plates are

depicted in Figures 2 and 3. It is observed that the primary velocity field decreases throughout the boundary layer region on increasing of magnetic parameter whereas secondary velocity field attains maximum value at near plate and decays slowly to boundary layer region. The reason for reduction in velocity fields is Lorentz force, which has tendency to slow down the fluid motion throughout the boundary layer region.

Figures 4 and 5 show that primary and secondary velocities in the region near to the plate get speed up with the increasing values of surface acceleration parameter b and gradually the influence of b becomes negligible in the region far from the plate. This conveys that higher the fluid motion gets fast near to the moving plate due to higher plate velocity.

A raising nature in both the velocities on increasing porosity parameter is explored in the Figures 6 & 7. An expansion in porosity leads to a lessened obstruction in the flow regime which causes a lower resistance to the flow and it increase the momentum.

Figures 8 & 9 depict the primary and secondary velocities for both ramped temperature and isothermal plates for different values of Grashof number. It is notice that both the velocity fields raise as increasing the Grashof number. Gr signifies that the ratio of buoyancy to viscous force. The reason for acceleration of fluid motion is slow down the buoyancy force due to temperature difference.

Influence of mass Grashof number on velocities is depicted in figures 10 and 11. It is shown that the profiles of velocities are increased on rising values of Gc. It happens due to the mass buoyancy force, since it has a trend to boost up velocity profile.

For both ramped temperature and isothermal plates, the primary and secondary velocity profiles versus for various values of rotation parameter are plotted in Figures 12 and 13. It is noticed that from the Figures 12 and 13, the primary velocity field slow down and whereas secondary velocity profile raises as increasing the rotation parameter. The Coriolis force causes to get down primary flow direction and produces a cross flow which is termed as secondary flow.

It is perceived from Figures 14 &15 that primary and secondary velocities experience an enlargement when Hall parameter m increases. It is recognized that larger estimations of Hall parameter m decline effective conductivity and subsequently decrease the magnetic damping force consequently velocity components get accelerated. Indeed, the Hall effect balances the resistive influence of applied magnetic field to some extent.

It elucidated from figures 16-18 that both the velocities and temperature get retarded for increasing values of Prandtl number. It is the ratio of momentum to thermal diffusion. Increase in Prandtl number corresponds to stronger momentum diffusion and weaker thermal diffusion. Here weaker thermal dispersion dominant over the stronger momentum due to which lower temperature is noticed. For rising values of Pr the thickness of the fluid increases, as a result velocity of the fluid will be decreased.

It is identified from Figures 19-21 that the velocities and temperature get retarded on accelerating radiation parameter. Generally, the thermal radiation parameter causes a fall in the temperature due to a fall in the kinetic energy of the fluid particles. This results in a corresponding decrease in the fluid velocities.

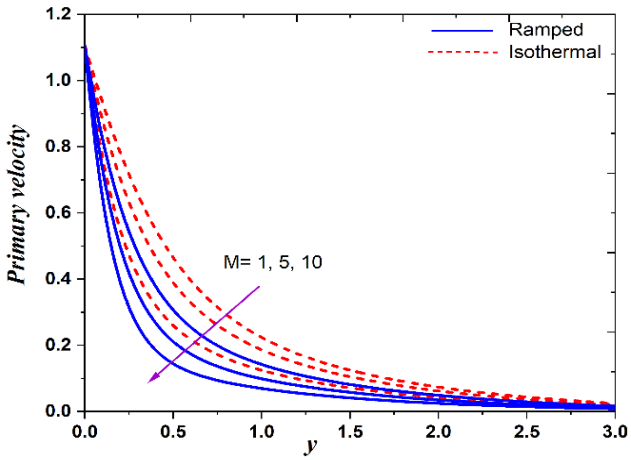

Figure-2. Primary velocity profile for M .

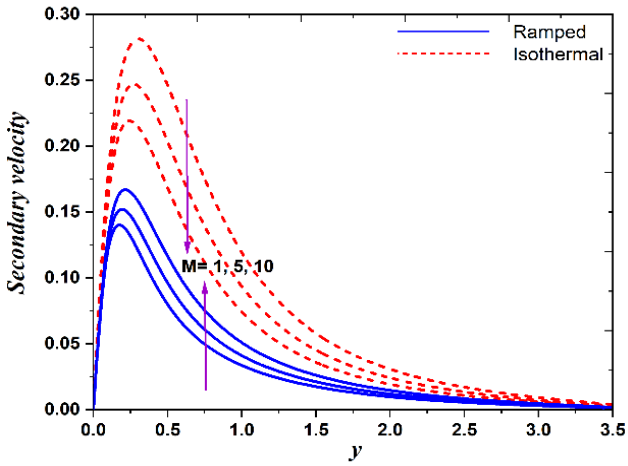

Figure-3. Secondary velocity profile for M .

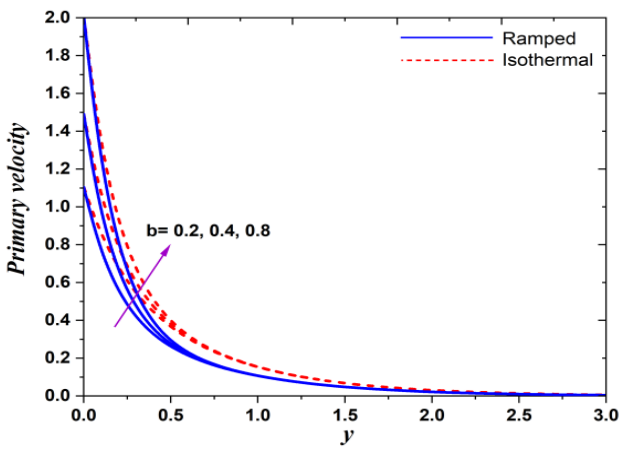

Figure-4. Primary velocity profile for b .

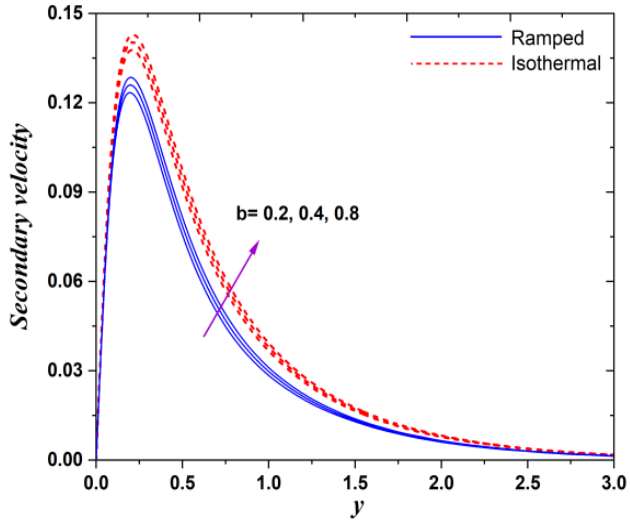

Figure-5. Secondary velocity profile for b.

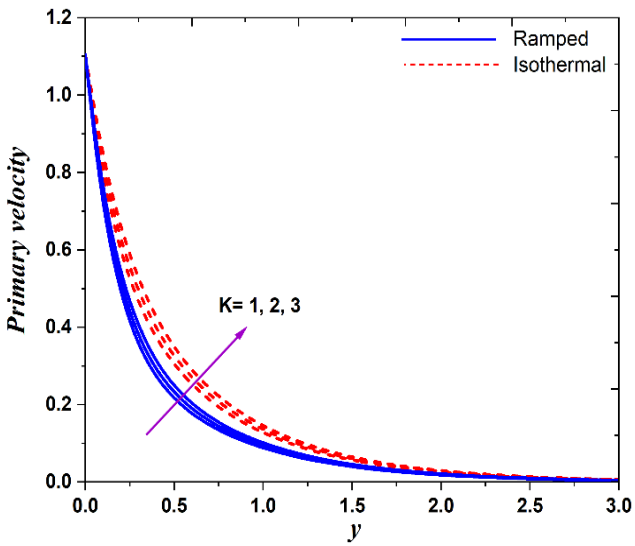

Figure-6. Primary velocity profile for K.

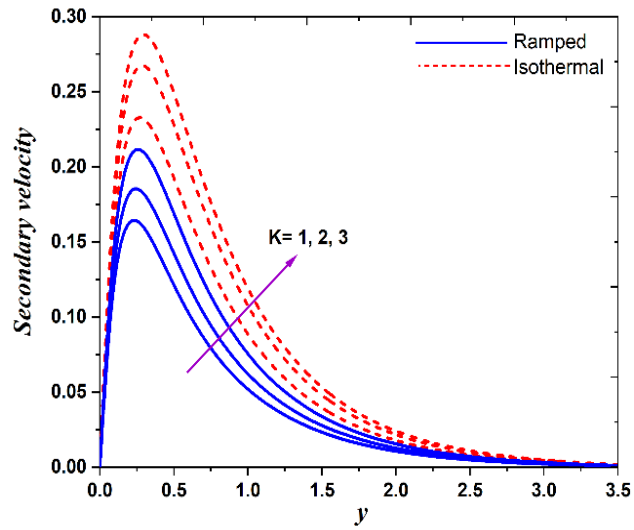

Figure-7. Secondary velocity profile for K.

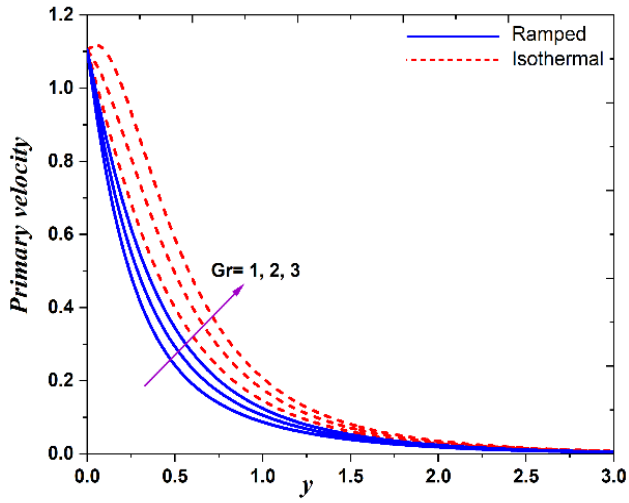

Figure-8. Primary velocity profile for Gr.

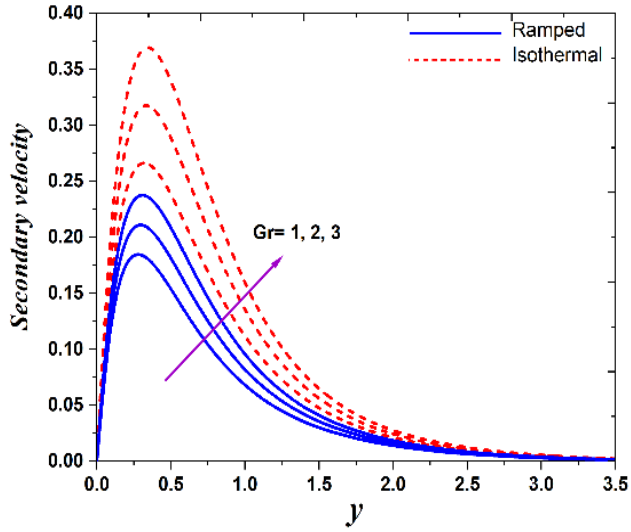

Figure-9. Secondary velocity profile for Gr.

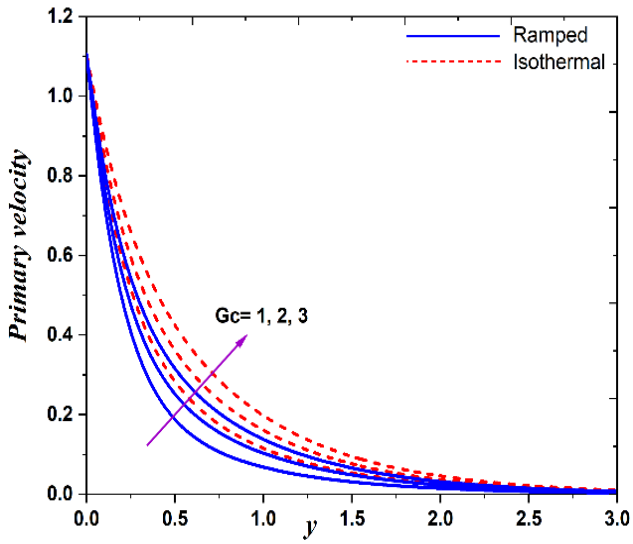

Figure-10. Primary velocity profile for Gc.

VOL. 16, NO. 18, SEPTEMBER 2021 ISSN 1819-6608
ARPN Journal of Engineering and Applied Sciences

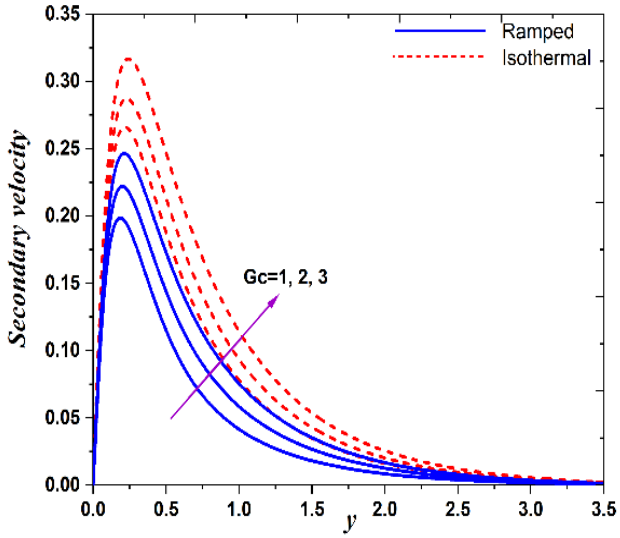

Figure-11. Secondary velocity profile for Gc.

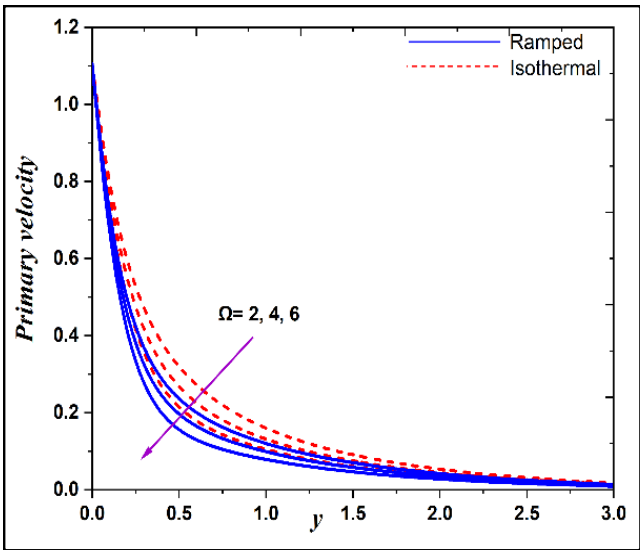

Figure-12. Primary velocity profile for Ω.

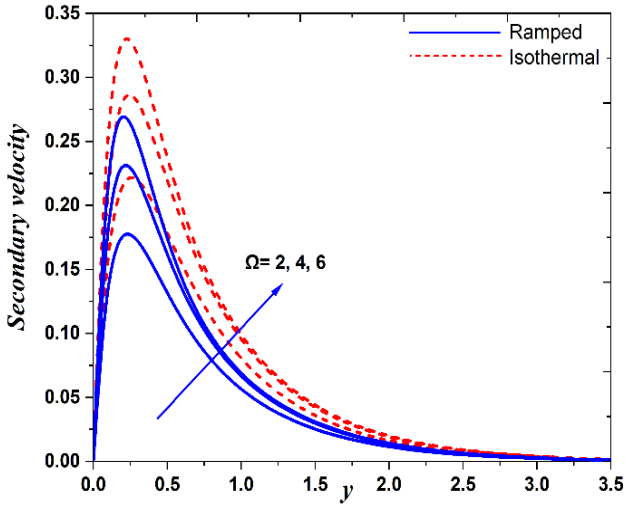

Figure-13. Secondary velocity profile for Ω.

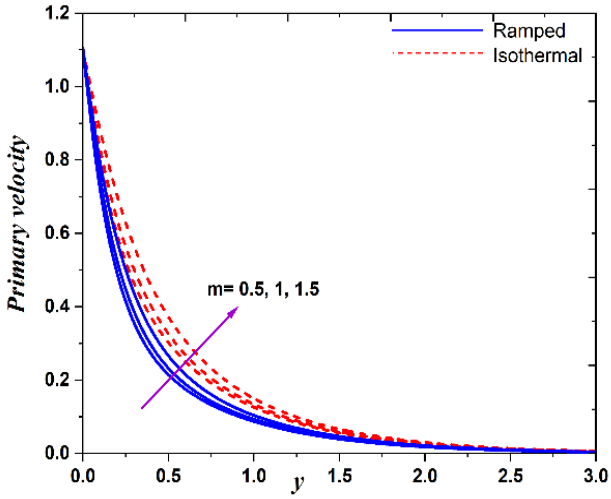

Figure-14. Primary velocity profile for m.

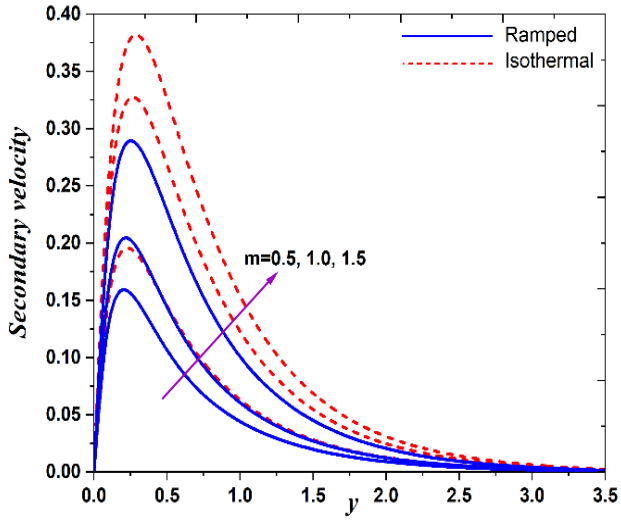

Figure-15. Secondary velocity profile for m.

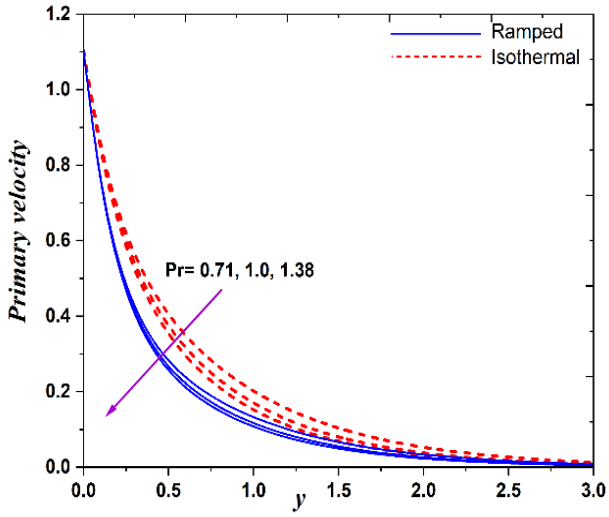

Figure-16. Primary velocity profile for $\Pr$.

VOL. 16, NO. 18, SEPTEMBER 2021 ISSN 1819-6608
ARPN Journal of Engineering and Applied Sciences

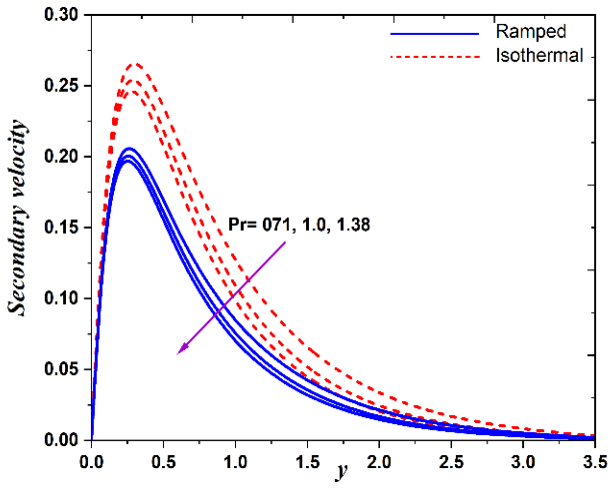

Figure-17. Secondary velocity profile for $\Pr$.

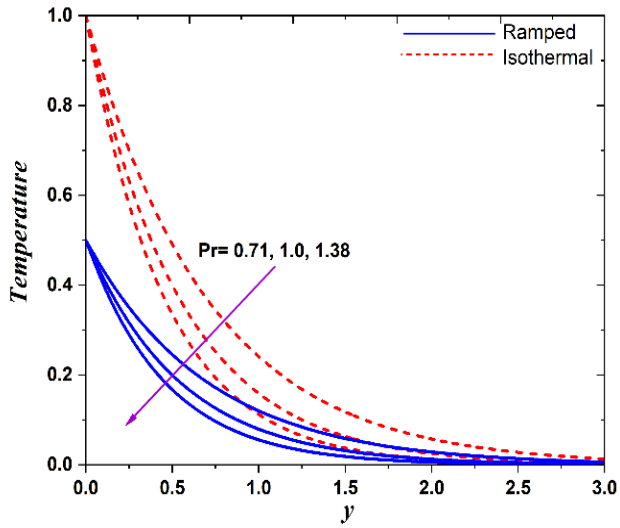

Figure-18. Temperature profile for $\Pr$.

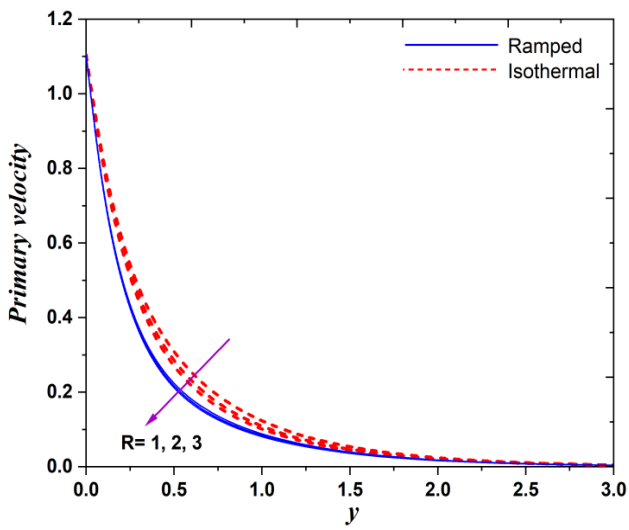

Figure-19. Primary velocity profile for R.

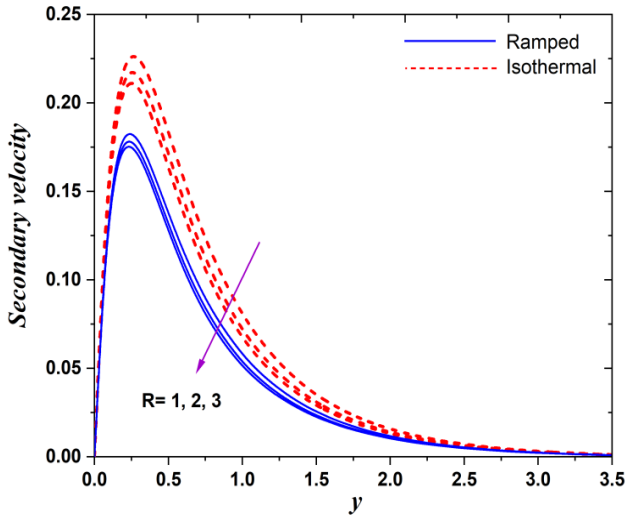

Figure-20. Secondary velocity profile for R.

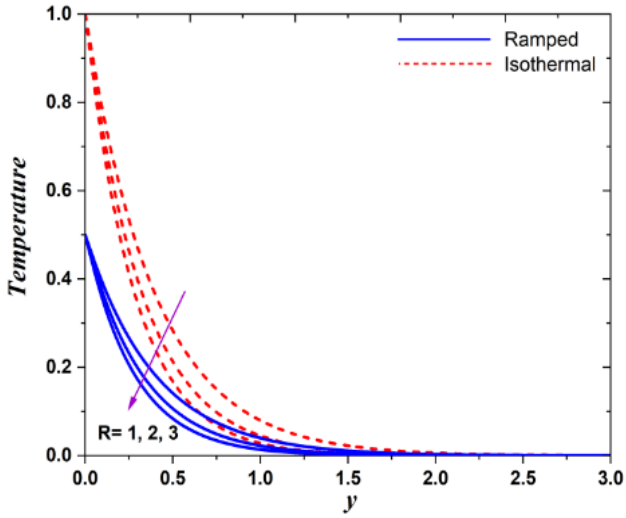

Figure-21. Temperature profile for R.

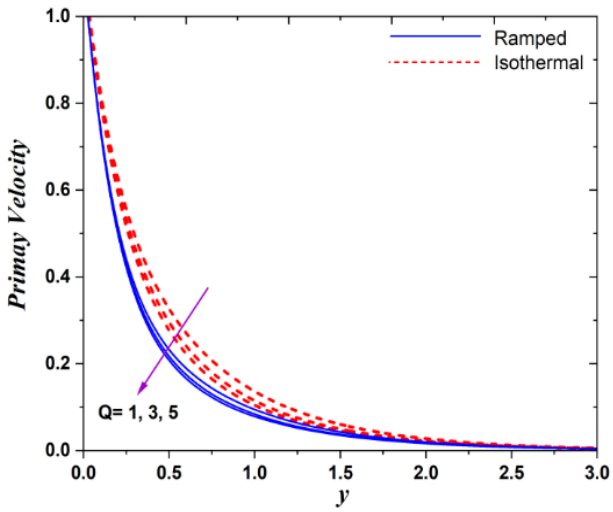

Figure-22. Primary velocity profile for Q.

VOL. 16, NO. 18, SEPTEMBER 2021 ISSN 1819-6608
ARPN Journal of Engineering and Applied Sciences

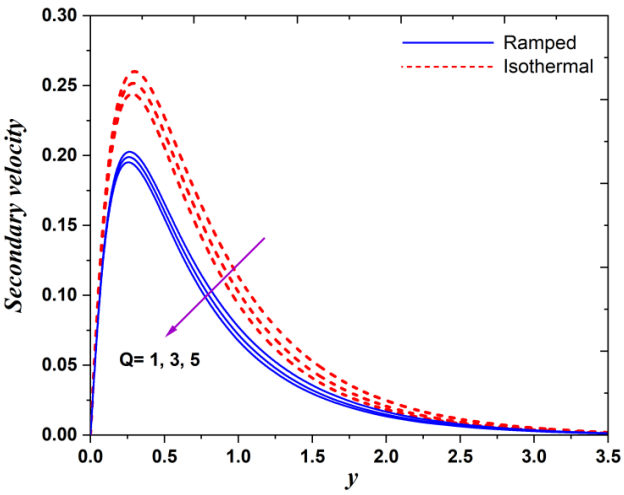

Figure-23. Secondary velocity profile for Q.

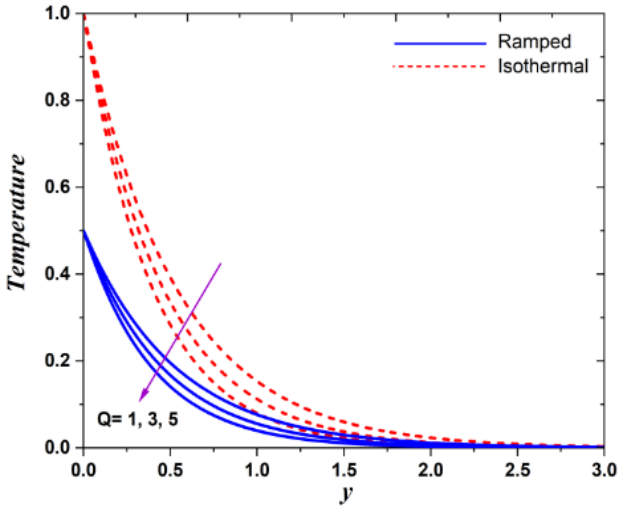

Figure-24. Temperature profile for Q.

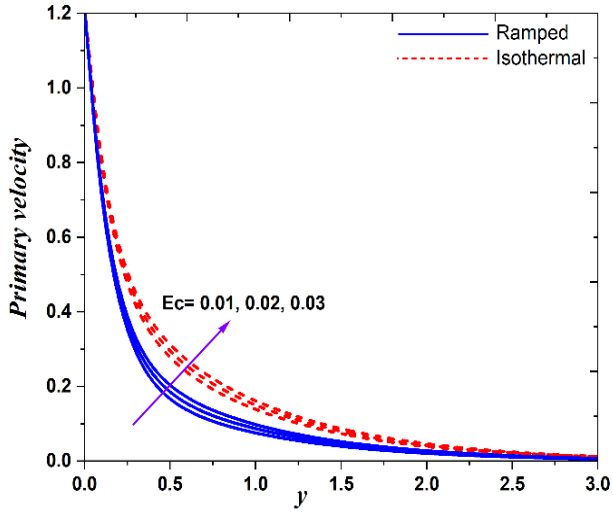

Figure-25. Primary velocity profile for Ec.

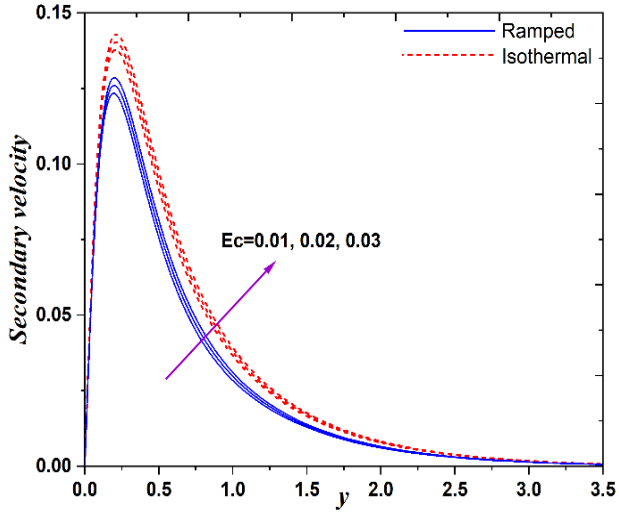

Figure-26. Secondary velocity profile for Ec.

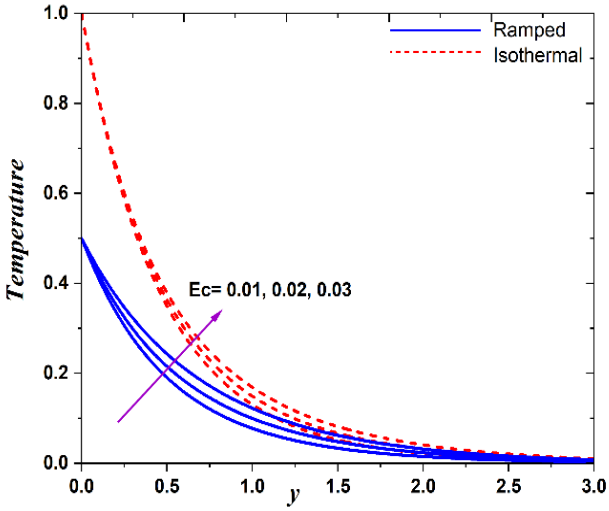

Figure-27. Temperature profile for Ec.

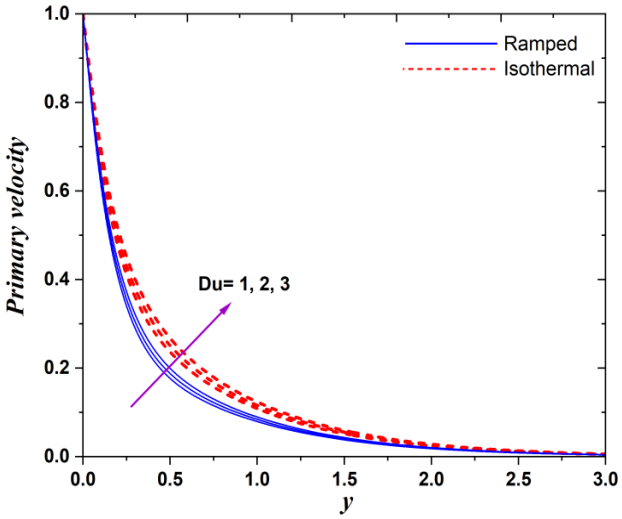

Figure-28. Primary velocity profile for Du.

VOL. 16, NO. 18, SEPTEMBER 2021 ISSN 1819-6608
ARPN Journal of Engineering and Applied Sciences

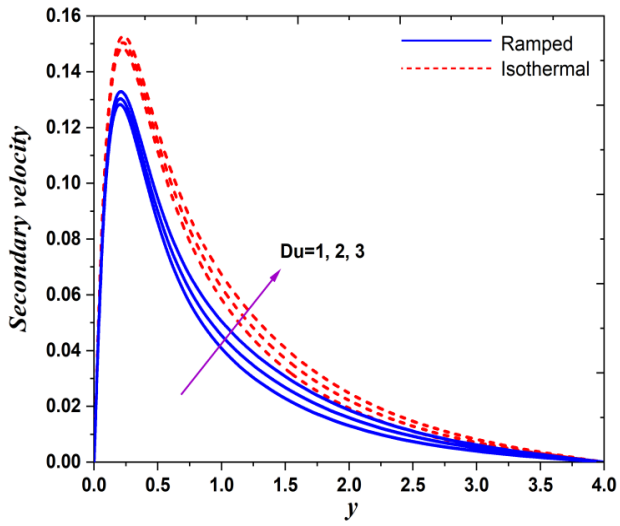

Figure-29. Secondary velocity profile for Du.

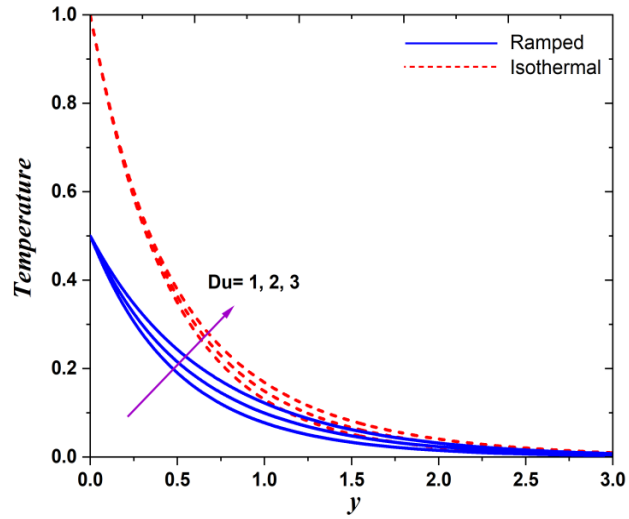

Figure-30. Temperature profile for Du.

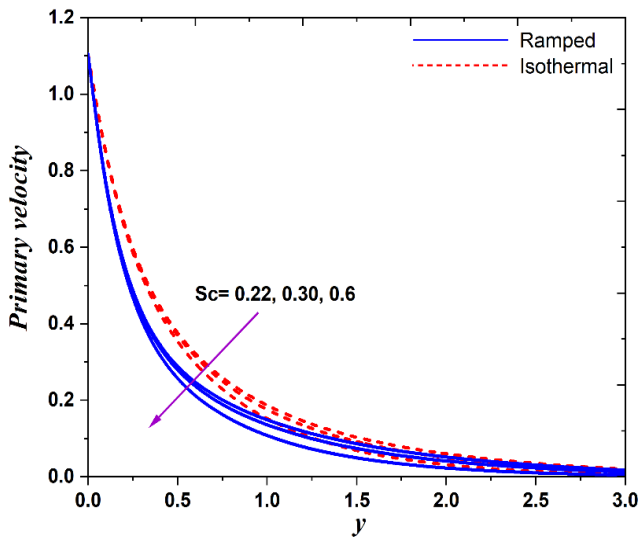

Figure-31. Primary velocity profile for Sc.

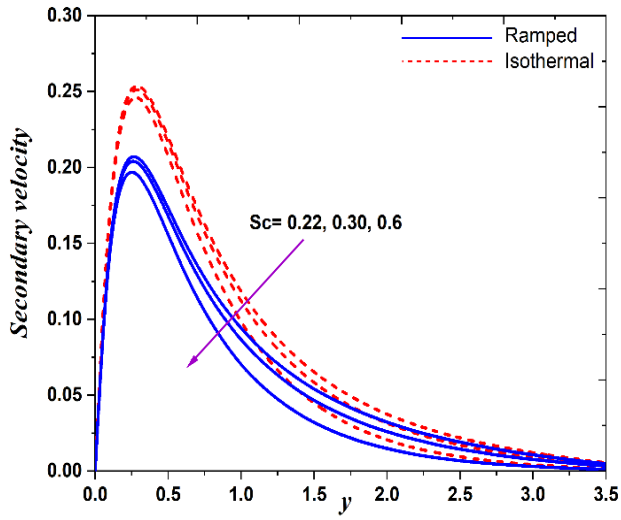

Figure-32. Secondary velocity profile for Sc.

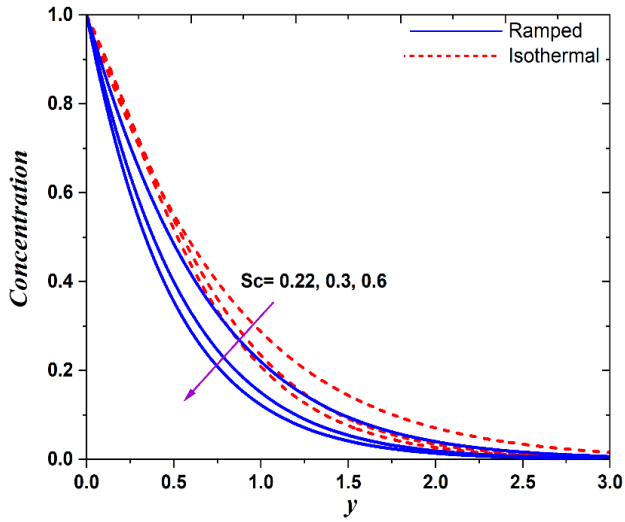

Figure-33. Concentration profile for Sc.

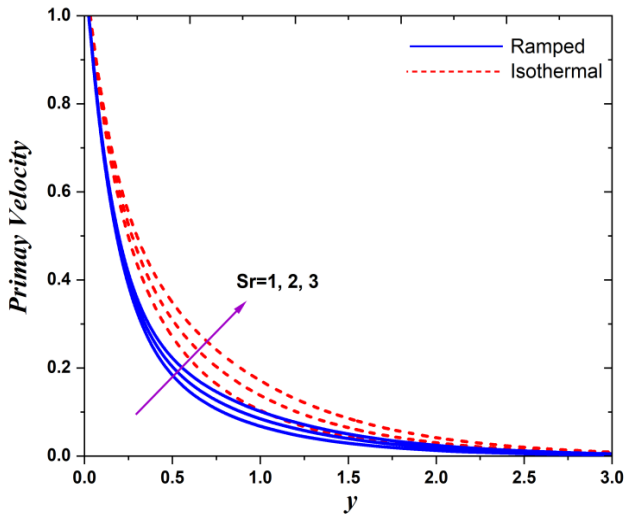

Figure-34. Primary velocity profile for Sr.

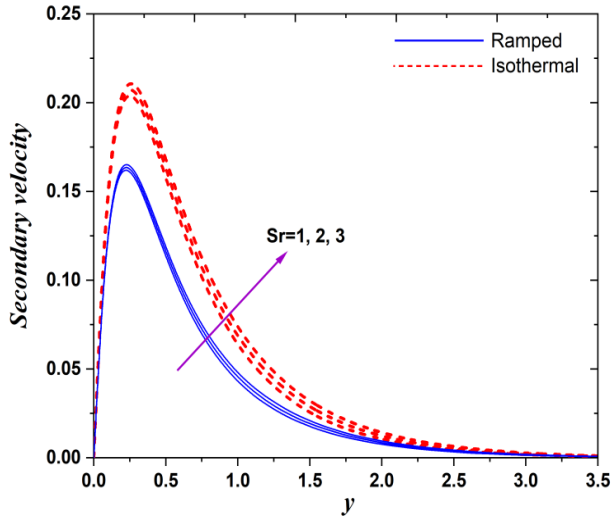

Figure-35. Secondary velocity profile for Sr .

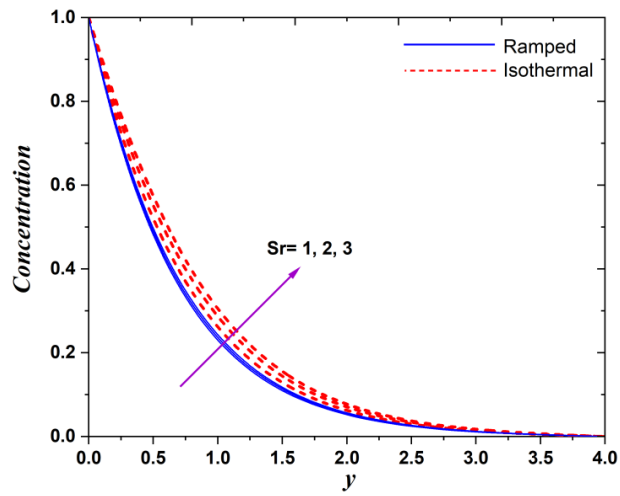

Figure-36. Concentration profile for Sr .

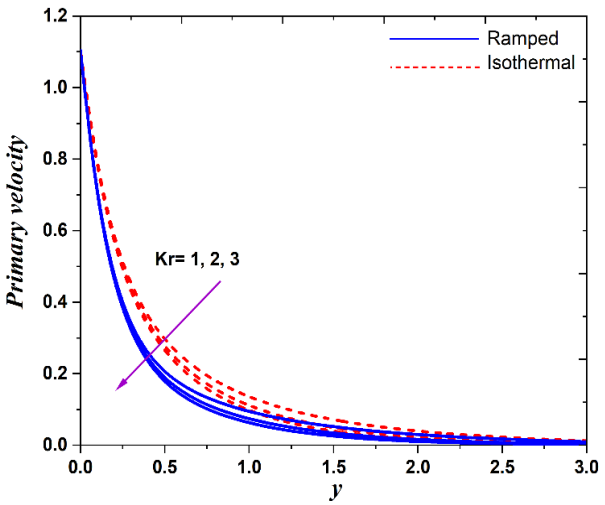

Figure-37. Primary velocity profile for Kr .

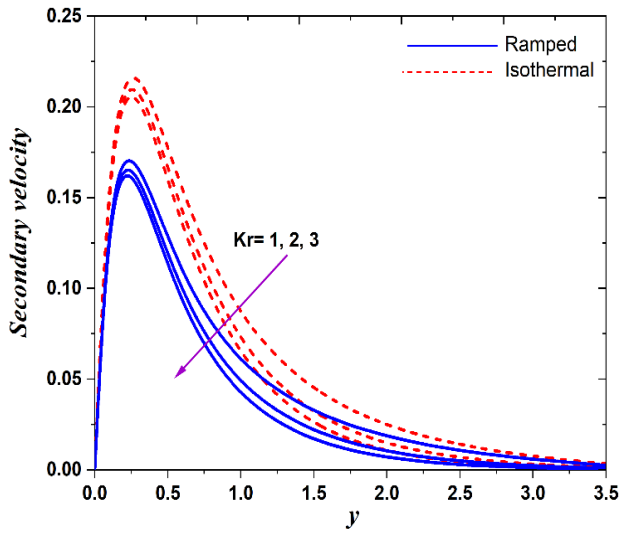

Figure-38. Secondary velocity profile for Kr .

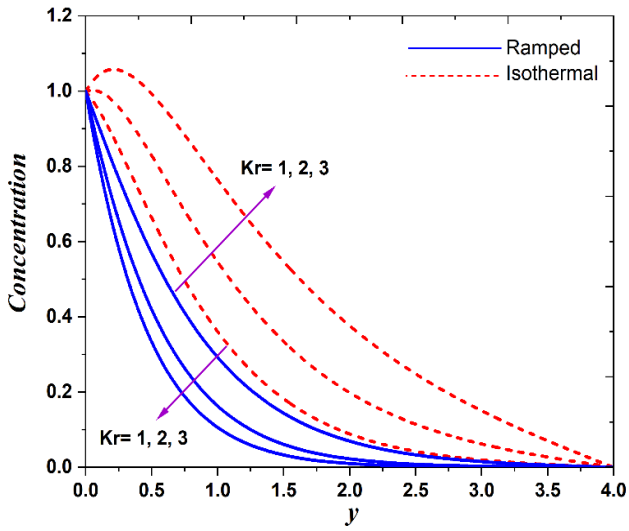

Figure-39. Concentration profile for Kr .

Figures 22-24 displays that both the velocities and temperature get decelerated on increasing heat absorption parameter. Since the heat absorption (thermal sink) effect has an attitude to reduce the fluid temperature and velocities.

The impact of the Eckert number on the velocities and temperature are appeared in Figures 25-27. Eckert number is the connection between kinetic energy in the stream and the enthalpy. It represents the change of kinetic energy into internal energy by work done against the viscous fluid stress. More noteworthy viscous dissipative heat causes an ascent in the temperature just as the velocities.

Figures 28-30 depict the variations in the velocities and temperature against Dufour number. Dufour number implies the contribution of the concentration gradients to the thermal energy flux in the stream. From figures, it is communicated that a development in the Dufour number causes a rising in the velocities and

temperature all through the boundary layer. It is seen that the temperature profiles break down easily from the plate to the free stream esteem. Be that as it may, a specific velocity overshoot exists near the plate, and from that point, the profile tumbles to zero at the edge of the boundary layer.

It is noticed from Figures 31-33 that, for both ramped temperature and isothermal plates, both velocity fields and concentration profiles decrease on increasing Sc. This implies that ratio of thermal and mass diffusion leads to slow down the velocity and concentration fields throughout the boundary layer region for both ramped temperature and isothermal plates.

The Soret number implies the contribution of the temperature gradients to the mass flux in the stream. It is clear from Figures 34 and 35 that the liquid speeds get revived by growing the Soret number, as an extension in the Soret number prompts a fall in the viscosity of the mixture. This causes a development in inertia impacts and a decrease in the viscous impacts. Thus, the speed parts increase. Figure-36 shows that the concentration profile increases with the development of the Soret number. A development in the Soret impact shows extending the molar mass dispersion, as seen from importance of Sr. The flood in the nuclear mass dispersion makes the concentration rise. This deduces the Soret number will as a rule upgrade the species concentration of the fluid.

The variety in both velocities and concentration profiles against chemical reaction is depicted in Figures 37-39. Figures 37 and 38 display that the two velocities get decelerated on rising chemical reaction parameter. Since concoction response boundary impacts the solute concentration which makes a decline in the liquid speed because of decreased mass buoyancy force. It is also observed from Figure-39 that concentration profile decreases on extending chemical reaction parameter. This is a direct result of the clarification that concoction response boundary affects the focus circulation of the stream field.

CONCLUSSIONS

The significant outcomes of the present study can be noted for both ramped temperature and isothermal plates as follows:

- As increasing the values of thermal Grashof number, mass Grashof number, Hall current parameter, rotation parameter, porosity parameter, surface acceleration parameter, Eckert number, Soret number and Dufour number the primary velocity profile increases. And found that is primary velocity decreases on increasing values of Prandtl number, thermal radiation, heat absorption, magnetic parameter, chemical reaction parameter and Schmidt number.

- Secondary velocity field raises as enhancing the thermal Grashof number, mass Grashof number, surface acceleration parameter, Hall current parameter, porosity parameter, Eckert number, Soret number and Dufour number. But secondary velocity field decreases as increasing Prandtl number, rotation parameter, thermal radiation, heat absorption, magnetic parameter, chemical reaction parameter and Schmidt number.

- Temperature profile decreases on rising the values of Prandtl number, thermal radiation and heat absorption and an opposite trend is identified against Eckert number and Dufour number.

- Concentration distribution diminishes on rising values of Schmidt number and chemical reaction parameter. A reverse phenomenon is recognized for enhancing the values of Soret number.

REFERENCES

[1] Beg OA, Ferdows M, Karim ME, Hasan MM, Beg TA, Shamshuddin M, Kadir A. 2020.Computation of non-isothermal thermo-convective micropolar fluid dynamics in a Hall MHD generator system with non-linear distending wall. International Journal of Applied and Computational Mathematics. 6(42): https://doi.org/10.1007/s40819-020-0792-y.

[2] Veeresh C, Varma S, Vijaya Kumar AG, Umamaheswar M, Raju MC. 2017. Joule heating and thermal diffusion effects on MHD radiative and convective Casson fluid flow past an oscillating semi-infinite vertical porous plate. Frontiers in Heat and Mass Transfer. 8(1): 1-8. https://doi.org/10.5098/hmt.8.1.

[3] Satya Narayana PV, Venkateswarlu B, Devika B. 2016. Chemical reaction and heat source effects on MHD oscillatory flow in an irregular channel. Ain Shams Engineering Journal. 7(4): 1079-1088. https://doi.org/10.1016/j.asej.2015.07.012.

[4] Makinde OD. 2012. Heat and mass transfer by MHD mixed convection stagnation point flow toward a vertical plate embedded in a highly porous medium with radiation and internal heat generation. Meccanica. 47(5): 1173-1184.https://doi.org/10.1007/s11012-011-9502-5.

[5] Bhaskar CV, Sheri SR, Suram, AK. 2018. MHD natural convection flow past a moving vertical plate with ramped temperature. ARPN Journal of Engineering and Applied Sciences. 13(22): 8846-8853.

[6] Bhaskar CV, Sheri S, Suram AK. 2020a. Finite element approximation of MHD flow past a vertical plate in an embedded porous medium with a convective boundary condition and cross diffusion. International Conference on Mathematical Sciences and Applications (ICMSA-2019) AIP Conference Proceedings. 2246: 020025-1-02002514.doi.org/10.1063/5.0015574.

[7] Bhaskar CV, Sheri S, Suram A. 2020b. Numerical analysis of MHD Casson fluid flow over an exponentially accelerated vertical plate in embedded porous medium with ramped wall temperature and ramped surface concentration in uniform magnetic field. International Journal of Applied Power Engineering (IJAPE). 9(89): 89-99. https://doi.org/10.11591/ijape.v9.i2.pp89-99.

[8] Jena S, Mishra SR, Dash G. 2016. Chemical Reaction effect on MHD Jeffery fluid flow over a stretching sheet through porous media with heat generation/absorption. International Journal of Applied and Computational Mathematics. 3:1225-1238.https://doi.org/10.1007/s40819-016-0173-8.

[9] Seth GS, Bhattacharyya A, Tripathi R. 2017. Effect of Hall current on MHD natural convection heat and mass transfer flow of rotating fluid past a vertical plate with ramped wall temperature. Frontiers in Heat and Mass Transfer (FHMT). 9(21): DOI: 10.5098/hmt.9.21.

[10] Bhargava R, Sharma S, Bhargava P, Bég OA, Kadir, A. 2017. Finite element simulation of nonlinear convective heat and mass transfer in a micropolar fluid-filled enclosure with Rayleigh number effects. International Journal of Applied and Computational Mathematics. 3(2): 1347-1379.https://doi.org/10.1007/s40819-016-0180-9.

[11] Pal D, Mondal H. 2011. MHD non-Darcian mixed convection heat and mass transfer over a non-linear stretching sheet with Soret-Dufour effects and chemical reaction. International Communications in Heat and Mass Transfer. 38(4): 463-467. https://doi.org/10.1016/J.ICHEATMASSTRANSFER.2010.12.039.

[12] Sheri S, Bhaskar CV, Suram A. 2020. Effect of viscous dissipation on natural convection flow past an impulsively moving vertical plate with ramped temperature. International Conference on Mathematical Sciences and Applications. (ICMSA-2019). AIP Conference Proceedings.2246:020007-1-020007-13.doi.org/10.1063/5.0014628

[13] Sheri SR, Reddy KR, Suram AK, Reddy MCK. 2018. Hall current and chemical reaction effects on free convective flow past an accelerated moving vertical plate with ramped temperature: FEM. ARPN Journal of Engineering and Applied Sciences. 13(6): 2017-2031.

[14] Siva Reddy Sheri, Chamkha Ali. J, Suram AK. 2017. Thermal-diffusion and diffusion-thermo effects on MHD natural convective flow through porous medium in a rotating system with ramped temperature. International Journal of Numerical Methods for Heat & Fluid Flow. 27(11): 2451-2480. https://doi.org/10.1108/HFF-09-2016-0349.

[15] Sheri SR, Suram, AK. 2016. Finite element analysis of heat and mass transfer past an impulsively moving vertical plate with ramped temperature.19:385–392. doi.org/10.6180/jase.2016.19.4.01.

[16] Mahendar D, Srikanth Rao P. 2015. Unsteady MHD free convection and mass transfer flow past a porous vertical plate in the presence of viscous dissipation. Journal of Physics: Conference Series. 66:1-6.

[17] Cramer KR, Pai SI. 1973. Magneto fluid Dynamics for Engineers and Applied Physicists, Mc Graw Hill Book Company, New York, USA.

[18] Raptis A. 2011. Free convective oscillatory flow and mass transfer past a porous plate in the presence of radiation for an optically thin fluid. Thermal Science, 15(3): 849-857. doi: 10.2298/TSCI101208032R.

[19] Bathe KJ. 2006. Finite Element Procedures, Prentice-Hall, New Jersey.

[20] Reddy JN. 2006. An Introduction to the Finite Element Method, McGraw-Hill Book Company, New York, 3rd Edition.